European Review for Medical and Pharmacological Sciences 2023; 27: 3979-3992

Empagliflozin and sacubitril/valsartan reverse methotrexate cardiotoxicity by repressing oxidative stress and hypoxia in heart embryonic H9c2 cardiomyocytes – the role of morphology of mitochondria observed on electron microscopy

Z. DOGAN[1], D.D. ERGUN[2], S. DURMUS[3], H. SAHIN[4], G.E. SENTURK[4], R. GELISGEN[3], A. SENYIGIT[5], H. UZUN[6]

[1]Department of Cardiology, Faculty of Medicine, Istanbul Atlas University, Istanbul, Turkey
[2]Department of Biophysics, Faculty of Medicine, Istanbul Aydin University, Istanbul, Turkey
[3]Department of Medical Biochemistry, Cerrahpasa Faculty of Medicine, Istanbul University-Cerrahpasa, Istanbul, Turkey
[4]Department of Histology and Embryology, Cerrahpasa Faculty of Medicine, Istanbul University-Cerrahpasa, Istanbul, Turkey
[5]Department of Internal Medicine, Faculty of Medicine, Istanbul Atlas University, Istanbul, Turkey
[5]Department of Medical Biochemistry, Faculty of Medicine, Istanbul Atlas University, Istanbul, Turkey

Abstract. – OBJECTIVE: Oxidative stress and hypoxia play an important role in the pathogenesis of various cardiovascular diseases. We aimed to evaluate the effectiveness of sacubitril/valsartan (S/V) and Empagliflozin (EMPA) on hypoxia-inducible factor-1α (HIF-1α) and oxidative stress in H9c2 rat embryonic cardiomyocyte cells.

MATERIALS AND METHODS: BH9c2 cardiomyocyte cells were treated with methotrexate (MTX) (10-0.156 μM), empagliflozin (EMPA; 10-0.153 μM) and sacubitril/valsartan (S/V; 100-1.062 μM) for 24, 48 and 72 h. The half maximum inhibitory concentration (IC_{50}) and half maximum excitation concentration (EC_{50}) values of MTX, EMPA and S/V were determined. The cells under investigation were exposed to 2.2 μM MTX before treatment with 2 μM EMPA and 25 μM S/V. The cell viability, lipid peroxidation, oxidation of proteins and antioxidant parameters were measured while morphological changes were also observed by transmission electron microscopy (TEM).

RESULTS: The results showed that treatment with 2 μM EMPA, 25 μM S/V or their combination produced a protective effect against the reduction in cell viability caused by 2.2 μM MTX. While HIF-1α levels plunged to their lowest with S/V treatment, oxidant parameters dipped, and antioxidant parameters soared to their highest level with S/V and EMPA combination treatment. A negative correlation was found between HIF-1α and total antioxidant capacity in the S/V treatment group.

CONCLUSIONS: A significant decrease in HIF-1α and oxidant molecules together with an enhancement in antioxidant molecules and normalization of the mitochondria morphology as observed on electron microscopy in S/V and EMPA-treated cells were detected. Although S/V and EMPA have both protective effects against cardiac ischemia and oxidative damage, this effect may be increased more with S/V treatment alone compared to combined treatment.

Key Words:
H9c2 cardiomyocyte cells, Empagliflozin, Sacubitril/valsartan, Electron microscopy, Hypoxia-inducible factor-1α, Oxidative stress.

Introduction

Heart diseases remain a serious health problem worldwide. That is because when cardiomyocytes are irreversibly injured, they cannot regenerate since the myocardium lacks myogenic stem cells capable of replacing the cells it lost and the essential contraction function they perform. Instead, the cardiomyocytes that undergo necrosis due to infarction are replaced by non-contractile fibroblasts and collagen. As a result, regional contraction disorders occur in varying degrees (hypokinesia, akinesia, dyskinesia, etc.)[1].

Sacubitril/valsartan (S/V) is a combination of an angiotensin receptor blocker (valsartan) and a neprilysin inhibitor prodrug (sacubitril)[2].

Corresponding Author: Zeki Dogan, MD; e-mail: drzeki@yahoo.com

Empagliflozin (EMPA), dapagliflozin, canagliflozin, and ertugliflozin, on the other hand, are selective inhibitors of sodium-glucose co-transporter type-2 (SGLT-2) used in the treatment of type 2 diabetes mellitus (T2DM), while sotagliflozin is an inhibitor of both SGLT-1 and 2[3]. European Society of Cardiology (ESC) guidelines[4] recommend those SGLT inhibitors, primarily empagliflozin among them, as the first choice in the treatment of T2DM in patients with cardiovascular diseases (CVD) for their positive cardiovascular effects.

In hypoxic conditions, two main signaling systems are activated in the body: AMP activated protein kinase (AMPK) and hypoxia-inducible (HIF) factor pathways. When the intracellular ATP level decreases, the AMPK pathway is activated, inhibiting anabolic processes while accelerating catabolic processes. HIF plays a key role in the cellular response to hypoxia in all mammalian cells[5]. Even in the absence of hypoxic conditions, cells constantly synthesize and degrade the HIF-α protein[6].

There is a balance between reactive oxygen species (ROS) and "antioxidant system" in physiological circumstances. Some growth factors, hormones and neurotransmitters in the cell use ROS as second messengers. However, excessive production of ROS (often due to exposure to chemicals, UV, ionizing radiation, and bacterial/viral infections) disrupts the balance of the body. It can damage cellular proteins and lipids and initiate carcinogenic activity by forming inserts in DNA. Not only ROS, but also the resulting oxidized lipid products [such as malondialdehyde (MDA) and 4-hydroxynonenal] lead to protein and DNA damage. This condition is altogether called the "oxidative stress". Increased oxidative stress has been viewed[7] as one of the potential common etiologies in various CVD. Previously, it has been reported that S/V and EMPA protect the cellular antioxidant defense system against oxidative stress by reducing lipid peroxidation activity in heart failure, myocardial infarction, and diabetic cardiomyopathy as shown in experimental and human studies[8-16]. Although S/V and EMPA reduce oxidative stress pathways in endothelial and cardiac cells[17,18], the exact underlying mechanisms remain unclear to this day.

In this study, the effects of S/V and EMPA on cell viability and also on HIF-1 in relation to inflammatory pathways during cell death in cells under hypoxic conditions, oxidative stress-activated lipid peroxidation, oxidation of proteins, and antioxidant in H9c2 cardiomyocyte cells were investigated. The results separately obtained were eventually compared with each other to draw a more reliable conclusion as to the effect of each agent, and that of their combined use.

Materials and Methods

All chemicals used in the study were provided by Sigma-Aldrich, Istanbul, Turkey.

Cell Culture Model

The study was conducted using H9c2 (2-1) cardiomyocyte cell line [The American Type Culture Collection (ATCC), Manassas, VA, USA]. The H9c2 cells were grown in high-glucose Dulbecco's modified Eagle's (DMEM; S.p.A.; Pero, Italy) supplemented with 10% heat inactivated fetal bovine serum (FBS; S.p.A.; Pero, Italy) and antibiotic solutions (100 U/mL penicillin and 100 U/mL streptomycin) (S.p.A.; Pero, Italy). The cells were seeded into 96-well plates (1x104 cells/well) and cultured in a humidified atmosphere at 37°C containing 5% CO_2. To investigate the effects of EMPA and S/V in MTX-induced H9c2 cells, the cells were incubated with MTX in complete culture medium for 48 h prior to addition of EMPA, S/V or their combinations.

Cell Viability Assay

In order to assess cell viability, proliferation, and cytotoxicity, the 3-(4,5-dimethylthiazol-2-yl)-2,5-diphenyltetrazolium bromide (MTT) test is employed to quantify cellular metabolic activity. This colorimetric assay relies on metabolically active cells to convert the yellow tetrazolium salt MTT to purple formazan crystals. The NAD(P)H-dependent oxidoreductase enzymes in the live cells convert MTT to formazan. Using a solubilization solution to dissolve the insoluble formazan crystals, the colored solution is then analyzed by measuring its absorbance with a spectrophotometer. The reference is that there are more metabolically active, viable cells in a solution that is darker[19,20].

H9c2 (2-1) cardiomyocyte cells were treated with different concentrations of methotrexate (MTX, Submex; Abdi Ibrahim, Istanbul, Turkey) (10-0.156 μM) and empagliflozin (Jardiance, Boehringer Ingelheim, Frankfurt, Germany) (10-0.153 μM) and sacubitril/valsartan (S/V, Novartis, Basel, Switzerland) (100-1.062 μM) for 24, 48 and 72 h at 37°C in a humidified atmosphere

containing 5% CO_2. MTX stock solution was diluted with 1% dimethyl sulfoxide (DMSO). EMPA and S/V were dissolved in DMSO. Final concentrations of all drugs were prepared in cell medium containing a non-toxic ratio of DMSO (≤ 0.05%). MTT colorimetric assay (Merck KGaA, Darmstadt, Germany) was used to evaluate cell viability. The medium was removed, and 100 µL DMEM and 20 MTT (5 mg/mL) were added to each well for 3 h. The formazan crystals that formed in intact cells were dissolved in 100 µL DMSO. Absorbance was recorded at a wavelength of 490 nm, and at a reference wavelength of 570 nm, using a microplate reader (Multiskan GO-Thermo, Waltham, MA USA). Using optical density (OD), the half maximum inhibitory concentration (IC_{50}) and half maximum excitation concentration (EC_{50}) values for MTX, EMPA and S/V were calculated for each incubation time (24 h, 48 h, and 72 h) with the GraphPad Software Prism ver. 9 (San Diego, CA, USA). 2.2 µM MTX, 2 µM EMPA and 25 µM S/V were used for 48 h. The cell viability was calculated by considering the control as 100%.

Cell Lysate Preparation

Using 1xRipa lysis buffer and a protease inhibitor cocktail set (Merck KGaA, Darmstadt, Germany), a cell lysate from all groups was created at the conclusion of the experiment. 300 µL of Ripa lysis buffer (0.5 M Tris-HCl, pH 7.4, 1.5 M NaCl, 2.5% deoxycholic acid, 10% NP-40, 10 mM EDTA) together with a protease inhibitor cocktail (1:200) were added after the cells have been washed twice with cold 1xPBS. The cells were blasted by pipetting on ice, and the cell suspension was incubated for 30 min at +4°C in a shaking water bath. It was then centrifuged at 14,000 xg for 30 min at +4°C. After centrifugation, the supernatants were transferred to fresh eppendorf tubes, and the resulting cell lysates were kept in a deep freezer at -80°C until measurement.

Transmission Electron Microscopic Examination

H9c2 (2-1) cardiomyocyte cells were seeded in 6-well plates at a density of 3 x 10^5 cells per well and experimental groups were designed. After that, the cells were treated with 0.25% Tripsin-EDTA for the dissociation from the surface of the well plates and were washed with PBS. Next, the cells were fixed with 2.5% glutaraldehyde for 1 hour at 4°C. Afterwards, glutaraldehyde was replaced by PBS and the cells were post-fixed with osmium tetroxide. The cells were incubated with grading ethyl alcohol series (50%, 70%, 80%, 90%, 96%, and 100%) for dehydration process after the embedding in 2% agar. The cells were exposed to propylene oxide, propylene oxide-araldite mix, and araldite solutions, respectively, for embedding in araldite blocks. Finally, polymerization was performed at 60°C for 48 hours. Semi-thin sections were taken from araldite blocks by ultramicrotome (Reichert UM3, Germany). Then thin sections were obtained on the copper grids and observed under TEM (JEOL, JEM-1011, Tokyo, Japan). The ultrastructural changes were observed in all experimental groups. Therefore, we focused on pseudopodia with membrane structures, mitochondria, cytoplasmic vacuoles, and endoplasmic reticulum (ER) dilatations of the cells.

Measurement of Hypoxia-Inducible Factor-1α (HIF-1α) Concentrations

Serum HIF-1α concentrations were measured by a commercially available sandwich enzyme linked immunoassay kit (Enzyme Linked Immunosorbent Assay, Cat No: E0422Hu, Bioassay Technology Laboratory, Shanghai, China). The coefficients of intra and inter assay variation were 6.9% (n = 25) and 8.9% (n = 25), respectively.

Measurements of Oxidative Stress Parameters

Lipoperoxidation of all samples was ascertained by the formation of MDA, which was estimated using the modified thiobarbituric acid (TBA) method[21]. Lipid hydroperoxide (LOOH) levels were determined spectrophotometrically according to the method of ferrous oxidation with xylenol orange version 2[22]. A modification of the Gelişgen et al[23] method was used for spectrophotometric determination of concentration of advanced oxidation protein products (AOPPs). Xanthine oxidase (XO) activity was determined spectrophotometrically with xanthine and 100% trichloroacetic acid (TCA) solution, as introduced by Prajda and Weber[24]. Plasma total thiol (T-SH) concentration was determined by using 5,5'-dithiobis (2-nitrobenzoic acid) (DTNB) as introduced by Hu[25]. Catalase (CAT) activity was measured in terms of the extent of hydrogen peroxide breakdown, as catalyzed by the enzyme[26]. The non-enzymatic total antioxidant level (TAC) of samples was evaluated with the ferric reducing antioxidant power assay and was performed according to the protocol of Benzie and Strain[27]. Each experiment group was repeated at least three times.

Statistical Analysis

The distribution of all analyzed parameters was confirmed using the Shapiro-Wilk test. All parameters were normally distributed and expressed as mean ± standard deviation. One-way ANOVA and Tukey test as post-hoc were used in the comparison of groups. Correlation analysis was performed using Pearson's correlation analysis. A *p*-value below 0.05 was expressed as significant. All statistical analyses were carried out using Statistical Package for the Social Sciences (SPSS) v. 21.0 (IBM Corp., Armonk, NY, USA) package program.

Results

The cells exposed to MTX without any treatment had a decreased viability, while the cells treated with EMPA, and S/V showed an increase in cell viability (Figure 1). As shown in Figure 2, the treatment with 2 μM EMPA and 25 μM S/V and their combinations after exposure to 2.2 μM MTX was found to protect the cell from the detrimental effects of MTX exposure.

Oxidative stress markers (AOPP, MDA, LOOH and XO activity) and HIF-1α increased and antioxidant capacity markers (T-SH, CAT activity and TAC) decreased in MTX-exposed cells compared to control cells (Table I). Oxidative stress markers (AOPP, MDA, LOOH and XO activity) decreased and antioxidant capacity markers (T-SH, CAT activity and TAC) increased in cells treated with EMPA, S/V and their combination compared to control cells (Table I). Compared to cells only exposed to MTX without treatment by any agent, oxidative stress markers (AOPP, MDA, LOOH, and XO activity) were decreased and antioxidant capacity markers (T-SH, CAT activity and TAC) increased in treated cells (Table II). In particular, the combined use of S/V and EMPA was more effective in decreasing oxidant markers and increasing antioxidant marker levels. As shown in Figure 3, there was a dramatic increase in HIF-1α levels in cells exposed to MTX. HIF-1α levels were found to be lower in healthy cells treated with EMPA and S/V compared to control. Cells treated with EMPA+S/V had similar levels to control. After exposure to MTX, HIF-1α levels were found to be significantly lower in cells treated with EMPA, S/V and EMPA+S/V compared to cells only exposed to MTX without receiving any treatment. The most effective decrease in HIF-1α levels was detected in cells treated with S/V. In the results of the correlation analysis, a significant negative correlation was found between HIF-1α and TAC levels in the groups treated with S/V (both healthy and those with S/V treatment, both MTX+S/V group and MTX+EMPA+S/V group) (Figure 4).

Morphologically, the ultrastructure of the control group revealed abundant granules while the nuclei were in a normal rounded shape with other organelles such as mitochondria, rough/smooth endoplasmic reticulum, and ribosomes. Pseudopodes were also seen in large numbers in the control group. On the other hand, the EMPA group showed many cells with the signs of nuclear fragmentation along with a large number of cytoplasmic vacuoles. Pseudopods were also observed to be shortened in the EMPA group. Interestingly, both EMPA+S/V and S/V groups demonstrated similar ultrastructural features compatible with the healthy cell structure. However, we realized that those groups had lower granules when we compared them to the control group (Figure 5).

Besides, some pyknotic cells were recognized when we observed the MTX group. The cells also showed severe nuclei fragmentation and contained many cytoplasmic vacuoles in this group. However, the cells from the MTX group demonstrated a lack of granules in their cytoplasm as well as decreased pseudopods. On the other hand, the cells from MTX+S/V group demonstrated more cytoplasmic vacuoles and peripherally located elongated mitochondria. Additionally, increased and branched pseudopods were seen in those cardiomyocytes belonging to the MTX+S/V group. In contrast, poorly developed pseudopods were seen in cardiomyocytes from the MTX+EMPA+S/V group. Moreover, the crista of the mitochondria was damaged, and their numbers were decreased similar to the MTX+EMPA group (Figure 6).

Discussion

Sacubutril/valsartan (S/V) is a molecule approved for the treatment of symptomatic low ejection fraction heart failure (HF)[28]. As an SGLT-2 inhibitor, EMPA can be used for a new class of anti-diabetic therapy and has been suggested[29] to have important preventive effects, especially for HF. In a study[30] investigating the cardioprotective effect of EMPA, it was observed that EMPA treatment increased cell viability in H9c2 cells exposed to hypoxia/reoxygenation. S/V, an angiotensin receptor-neprilysin inhibitor, was observed[31] to protect against

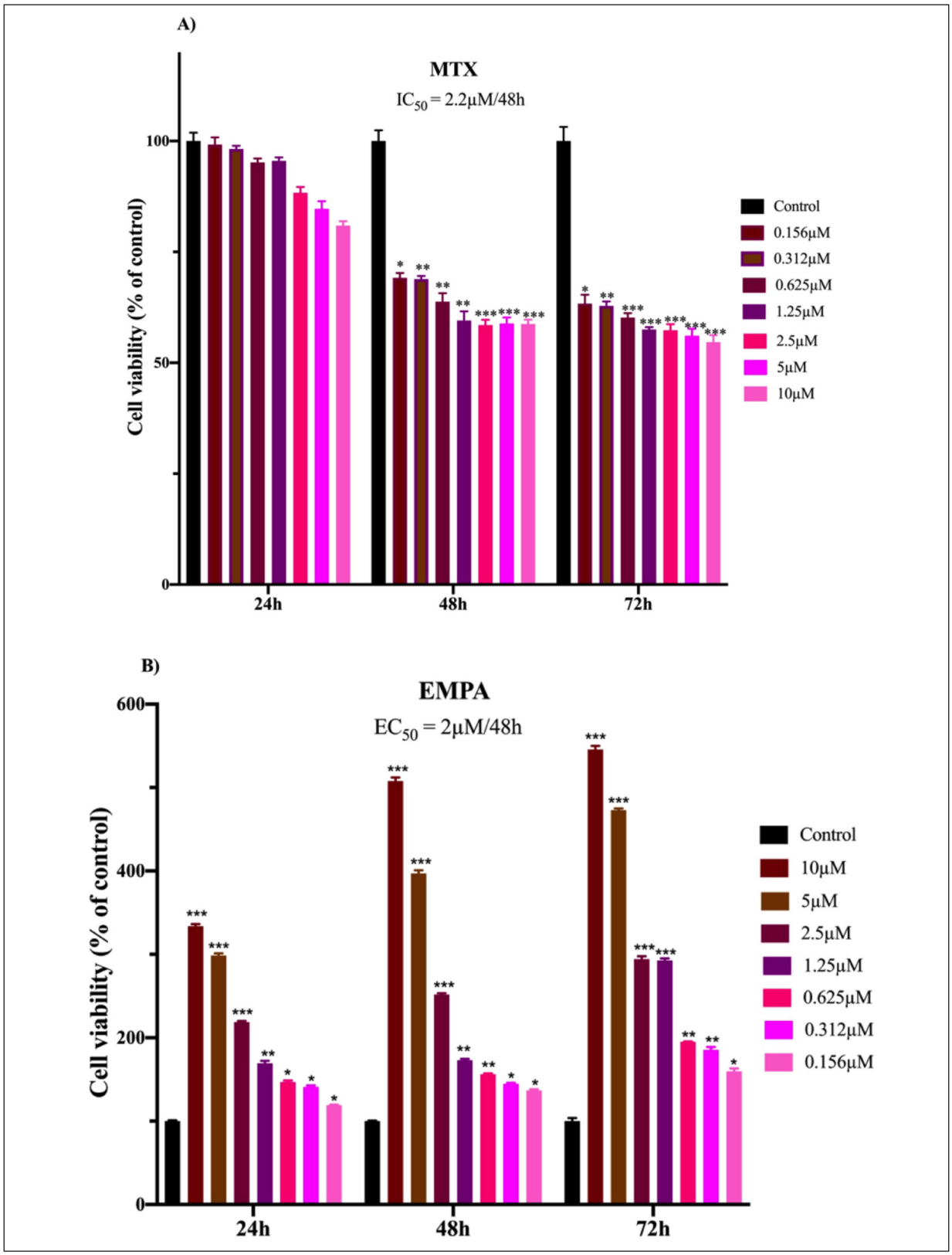

Figure 1. A-B, Time- and dose-dependent effects of (**A**), MTX, (**B**), EMPA and (**C**), S/V in cell viability in H9c2 cells as % of control. Data are presented as the mean ± standard error of the mean (n = 6). MTX: Methotrexate; EMPA: Empagliflozin; S/V: Sacubitril/valsartan. *$p < 0.05$; **$p < 0.01$; ***$p < 0.001$; *vs.* control.

Figure continued

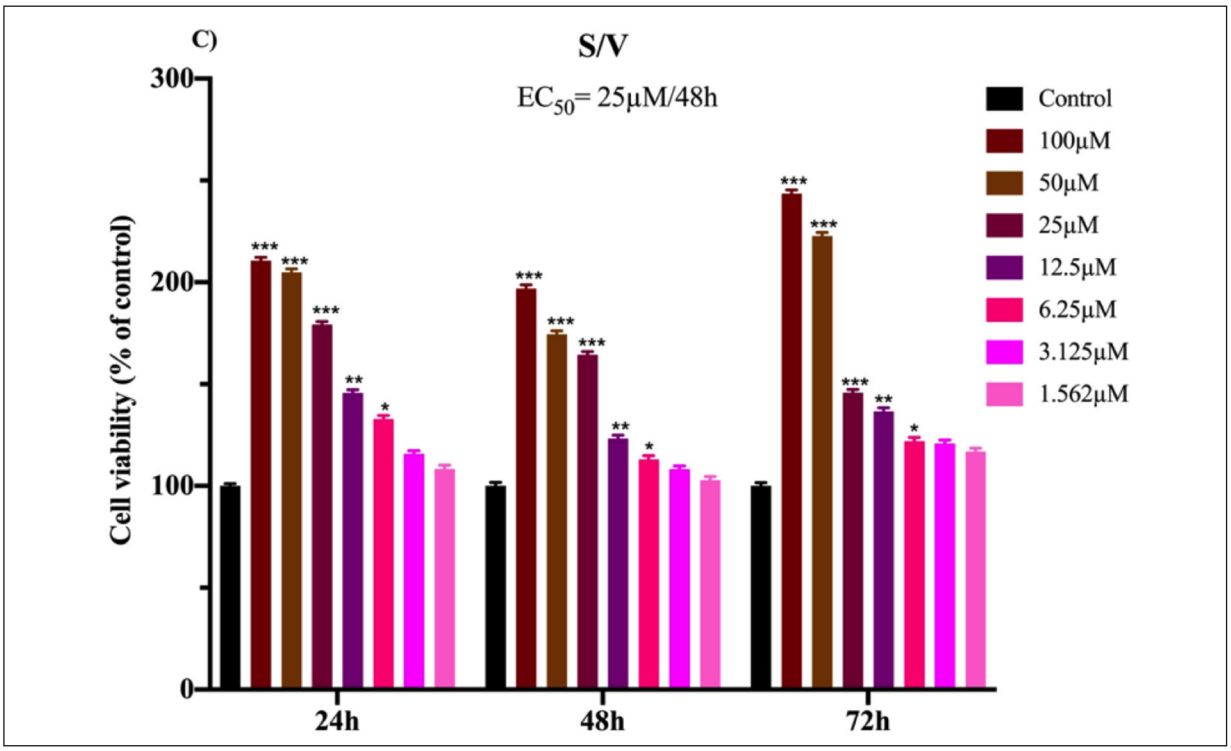

Figure 1 ***(Continued).*** **C**, S/V in cell viability in H9c2 cells as % of control. Data are presented as the mean ± standard error of the mean (n = 6). MTX: Methotrexate; EMPA: Empagliflozin; S/V: Sacubitril/valsartan. *$p < 0.05$; **$p < 0.01$; ***$p < 0.001$; *vs.* control.

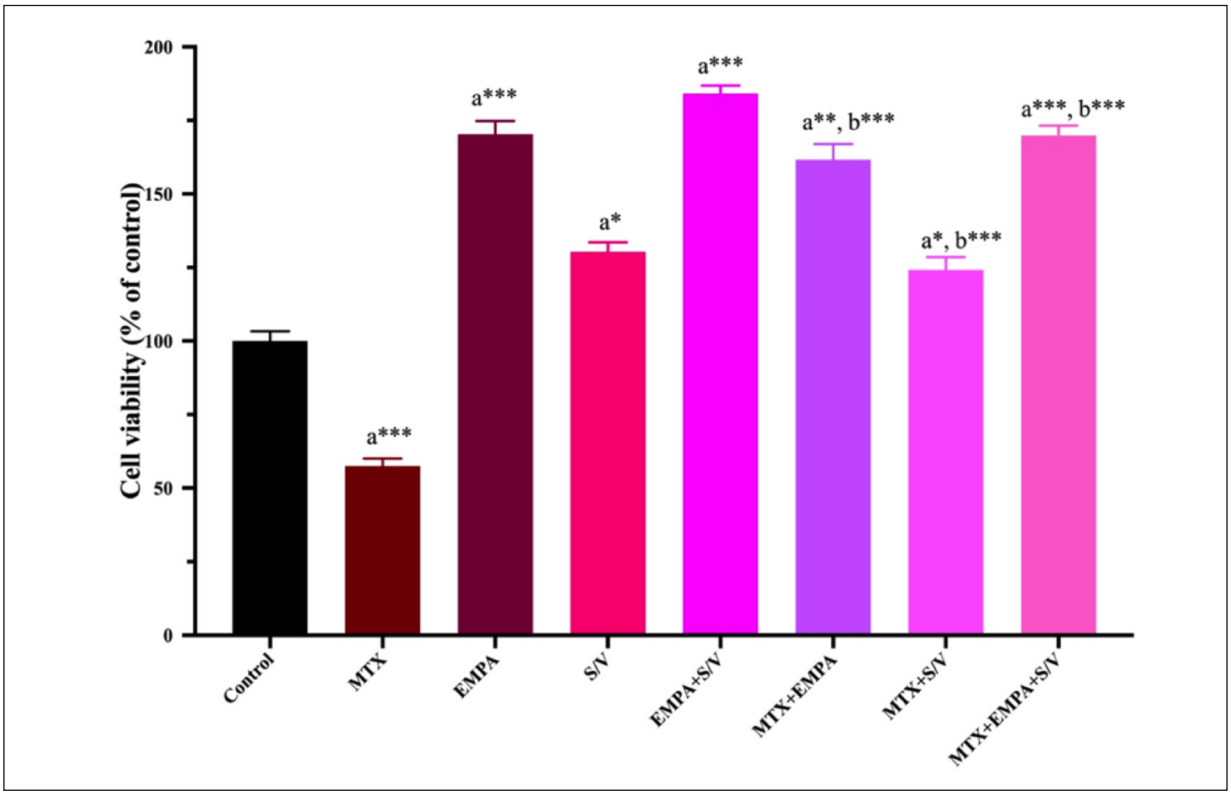

Figure 2. Protective effects of EMPA, S/V and their combinations against MTX-induced decrease in cell viability in H9c2 cells as % of control. Data are presented as the mean ± standard error of the mean (n = 6). MTX: Methotrexate; EMPA: Empagliflozin; S/V: Sacubitril/valsartan. *$p < 0.05$; **$p < 0.01$; ***$p < 0.001$; a: *vs.* control; b: *vs.* MTX.

Table I. HIF-1α levels, oxidant, pro-oxidant and antioxidant markers in H9c2 cardiomyocyte control cells, cells exposed to MTX without any treatment, and cells treated with EMPA, S/V and their combination.

	Control Mean ± S.D.	MTX Mean ± S.D.	EMPA Mean ± S.D.	S/V Mean ± S.D.	EMPA + S/V Mean ± S.D.
HIF-1α (ng/mL)	0.05 ± 0.01	0.31 ± 0.01^{a***}	0.03 ± 0.01^{a**}	0.02 ± 0.01^{a***}	0.05 ± 0.01
AOPP (μM chloramine-T equivalents)	90.17 ± 6.18	173.17 ± 10.21^{a***}	74.33 ± 2.66^{a***}	77.33 ± 3.56^{a***}	63.83 ± 2.93^{a***}
MDA (nmol/mL)	0.69 ± 0.1	0.88 ± 0.05^{a***}	0.59 ± 0.02^{a**}	0.64 ± 0.02	0.29 ± 0.04^{a***}
LOOH (nmol/mL)	13.2 ± 0.57	20.15 ± 1.01^{a***}	11.74 ± 0.71	12.65 ± 0.72	5.94 ± 0.16^{a***}
XO activity (mU/mg protein)	1.95 ± 0.14	2.71 ± 0.23^{a***}	1.27 ± 0.2^{a***}	1.62 ± 0.21^{a**}	1.03 ± 0.17^{a***}
T-SH (mM)	1.3 ± 0.14	0.79 ± 0.05^{a***}	1.83 ± 0.07^{a***}	1.65 ± 0.19^{a**}	2.14 ± 0.28^{a***}
CAT activity (U/mg Protein)	3.31 ± 0.49	2.53 ± 0.42^{a***}	4.62 ± 0.27^{a***}	3.94 ± 0.08^{a**}	7.16 ± 0.15^{a***}
TAC (μg ascorbic acid equivalent/mL)	17.54 ± 0.53	13.26 ± 0.53^{a***}	18.63 ± 0.41^{a**}	18.77 ± 0.51^{a**}	21.85 ± 0.9^{a***}

MTX: Methotrexate; EMPA: Empagliflozin; S/V: Sacubitril/valsartan; HIF-1α: Hypoxia-inducible factor 1-alpha; MDA: malondialdehyde; LOOH: lipid hydroperoxide; AOPP: advanced oxidation protein products; XO: xanthine oxidase; T-SH: total thiol; CAT: catalase; TAC: total antioxidant capacity. *$p < 0.05$; **$p < 0.01$; ***$p < 0.001$; ^{a}: *vs*. control.

doxorubicin-induced cardiotoxicity and increase cell viability. Cardiomyocyte cells are both protected by EMPA and S/V. We have shown that treatment with 2 μM EMPA, 25 μM S/V, or combinations thereof inhibit 2.2 μM MTX-induced cell toxicity as a measure of cell viability. In our cell culture study with cardiomyocyte cells, we observed that treatment with EMPA and S/V significantly improved the survival-cell viability of cardiomyocyte cells, and S/V treatment with EMPA protected cells in terms of total antioxidant capacity reduced by MTX.

Accordingly, in some pyknotic cells, many cytoplasmic vacuoles, decreased granules in cytoplasm and pseudopods may occur. Finally, the damaged mitochondria and cells can be eliminated by application of S/V, EMPA and their combinations, which elucidated the underlying mechanisms. Furthermore, the significant decrease in HIF-1α, MDA, LOOH, AOPP, XO activity and enhancement in T-SH, CAT and TAC in S/V and EMPA-treated cells were observed. The results suggest that S/V and EMPA protected the H9c2 cells under hypoxia and oxidative stress through inhibiting hypoxia and oxidative stress damage. Although S/V and EMPA both have protective effects on cardiac ischemia and oxidative damage, this effect may be increased more with S/V treatment compared to combined treatment.

While HIF-1α degrades rapidly in normoxia (21% oxygen), its degradation slows down when the oxygen concentration in the environment drops to 5%. For this reason, HIF measurement is accepted as an indicator of hypoxic conditions in *in vitro* studies[32,33]. As the severity of hypoxia increases and anoxia develops (0.1% oxygen), the level of HIF-1α protein also increases[32,34]. In

Table II. HIF-1α levels, oxidant, pro-oxidant and antioxidant markers in H9c2 cardiomyocyte cells exposed to MTX without any treatment, cells exposed to MTX treated with EMPA, S/V and their combination.

	MTX Mean ± S.D.	MTX + EMPA Mean ± S.D.	MTX + S/V Mean ± S.D.	MTX + EMPA + S/V Mean ± S.D.
HIF-1α (ng/mL)	0.31 ± 0.01	0.06 ± 0.01^{a***}	0.04 ± 0.01^{a***}	0.11 ± 0.01^{a***}
AOPP (μM chloramine-T equivalents)	173.17 ±10.21	83.33 ± 1.37^{a***}	84.33 ± 1.37^{a***}	74 ± 0.89^{a***}
MDA (nmol/mL)	0.88 ± 0.05	0.79 ± 0.02^{a**}	0.74 ± 0.02^{a***}	0.55 ± 0.03^{a***}
LOOH (nmol/mL)	20.15 ± 1.01	3.69 ± 1.52^{a***}	12.95 ± 1.15^{a***}	7.4 ± 0.57^{a***}
XO activity (mU/mg protein)	2.71 ± 0.23	2.08 ± 0.06^{a***}	2.08 ± 0.05^{a***}	1.39 ± 0.05^{a***}
T-SH (mM)	0.79 ± 0.05	1.18 ± 0.03^{a***}	1.12 ± 0.03^{a***}	1.81 ± 0.05^{a***}
CAT activity (U/mg Protein)	2.53 ± 0.42	3.73 ± 0.1^{a***}	3.92 ± 0.06^{a***}	5.2 ± 0.06^{a***}
TAC (μg ascorbic acid equivalent/mL)	13.26 ± 0.53	17.57 ± 0.21^{a***}	17.51 ± 0.2^{a***}	20.97 ± 0.1^{a***}

MTX: Methotrexate; EMPA: Empagliflozin; S/V: Sacubitril/valsartan; HIF-1α: Hypoxia-inducible factor 1-alpha; MDA: malondialdehyde; LOOH: lipid hydroperoxide; AOPP: advanced oxidation protein products; XO: xanthine oxidase; T-SH: total thiol; CAT: catalase; TAC: total antioxidant capacity. *$p < 0.05$; **$p < 0.01$; ***$p < 0.001$; ^{a}: *vs.* MTX.

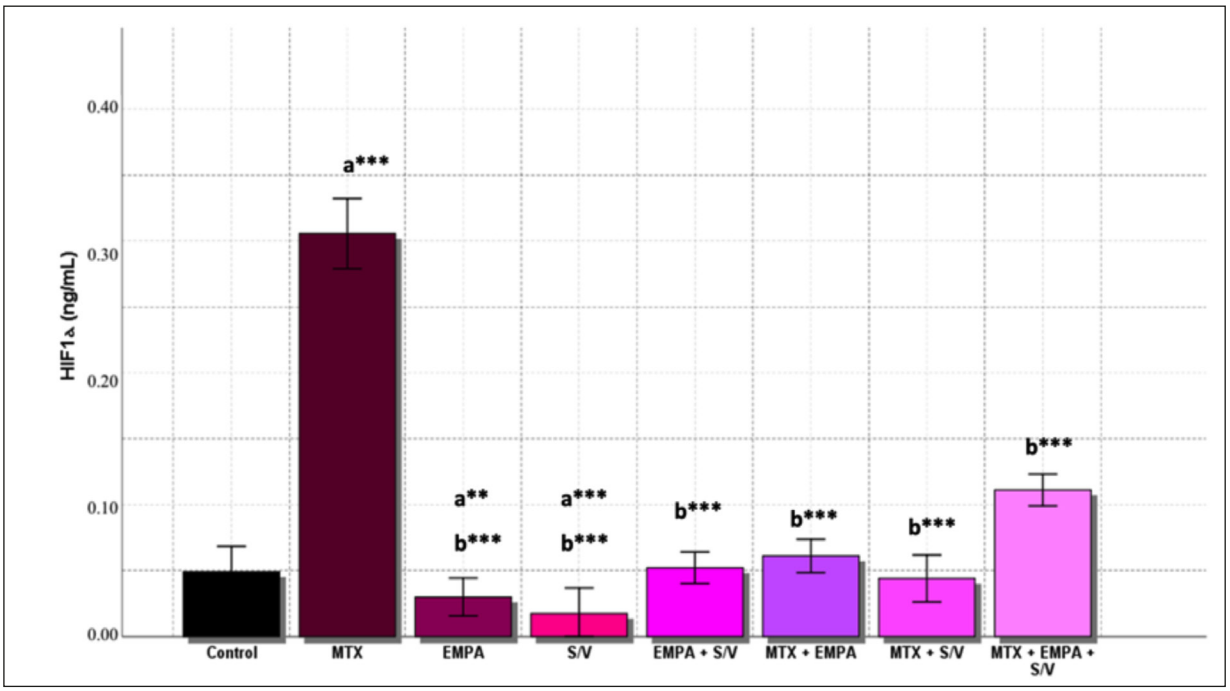

Figure 3. HIF-1α levels in H9c2 cardiomyocyte control cells, cells exposed to MTX without any treatment, and treated with only EMPA, S/V and their combination and cells exposed to MTX and treated with EMPA, S/V and their combination. a: *vs.* Control; b: *vs.* MTX.

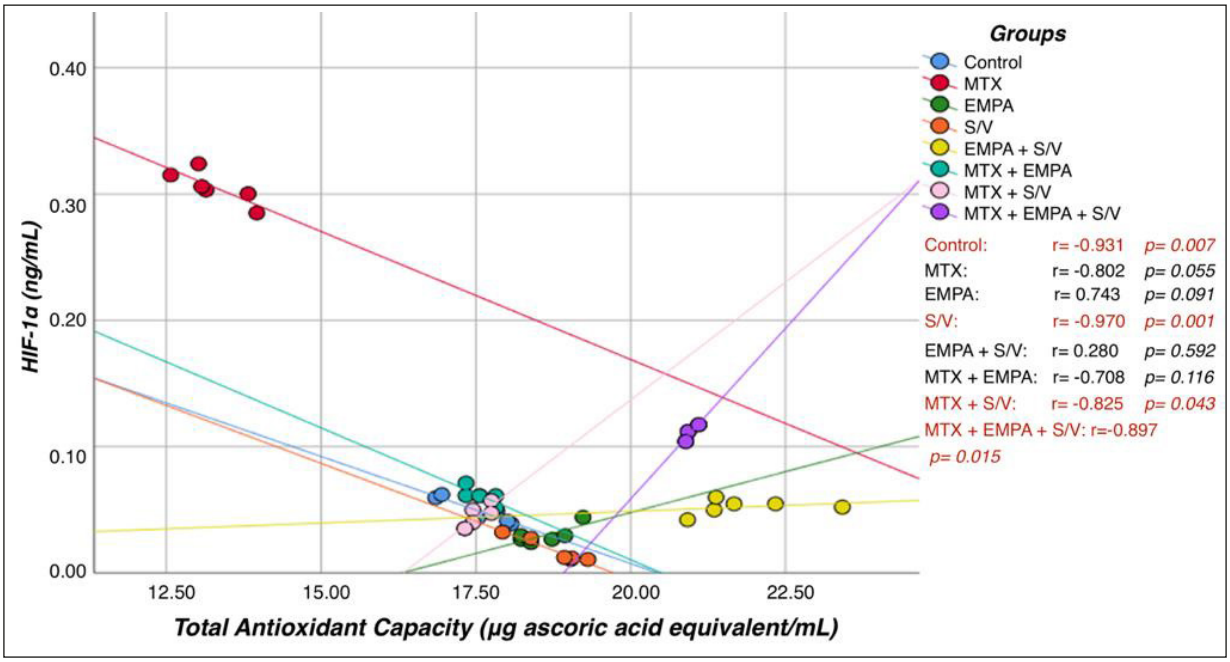

Figure 4. Pearson's correlation scatter plot of the H9c2 cells lysate level of HIF-1α and total antioxidant capacity in all groups. Written in red and bold indicate that statistically significant. A significant negative correlation was found between HIF-1α and TAC in the S/V treatment group, the MTX + S/V group, and the MTX + EMPA + S/V group.

our study, HIF-1α level was measured to show that the environment remains hypoxic at the cell level. HIF-1α levels were found to have increased in the MTX group in our study. These findings indicate that hypoxic conditions are established and maintained. HIF-1α is an essential protein for

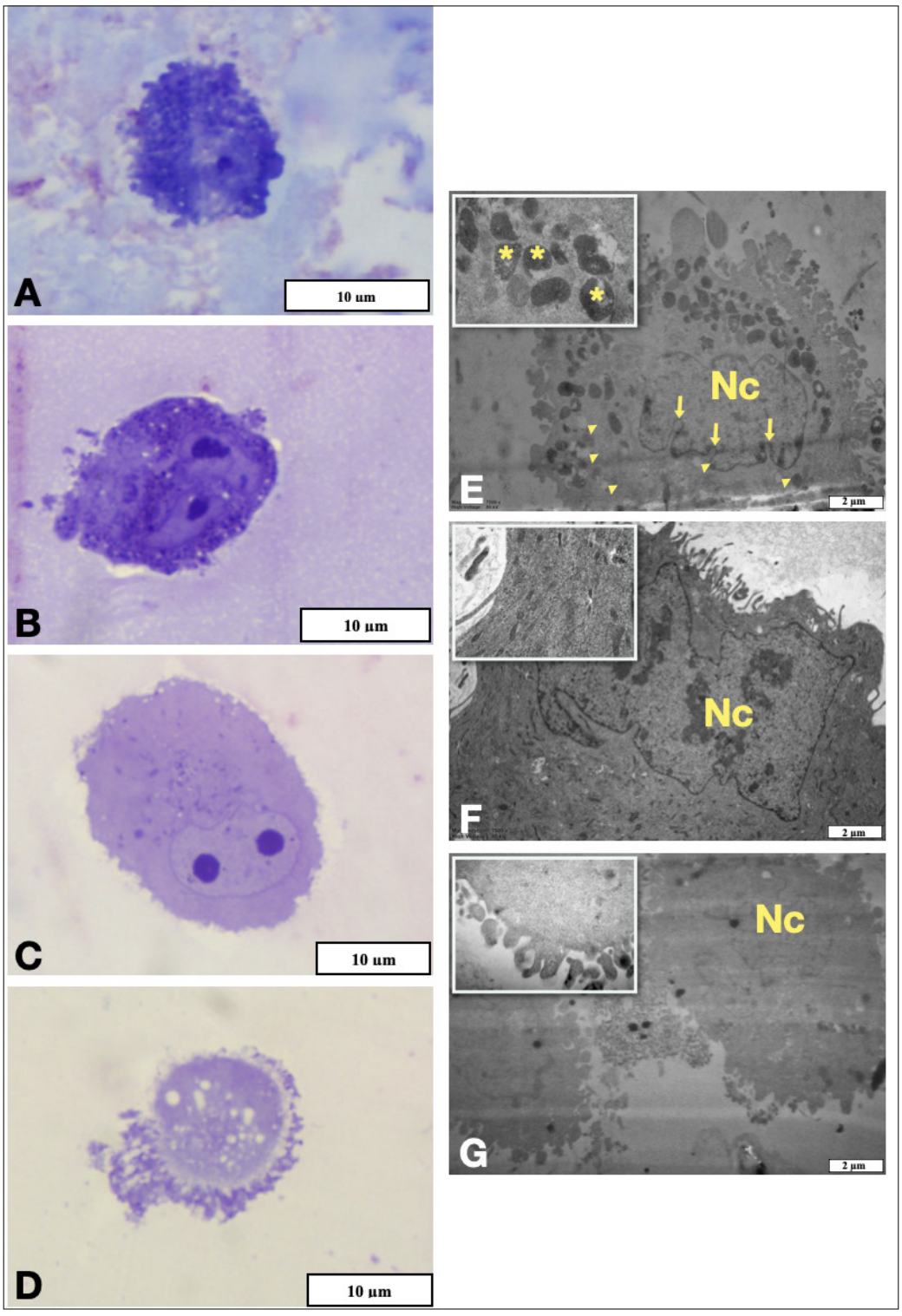

Figure 5. Representative micrographs from semi-thin (**A-D**) and thin (**E-G**) sections of the H9c2 (2-1) cardiomyocyte cell line. **A**, Control group showed a round nucleus with 1/2 nucleoli. The organelles related to protein synthesis were abundant. **B** and **E**, EMPA group showed nuclear fragmentation (arrow) andabundant from granules (asteriks) as seen in inset from (**E**). Many cytoplasmic vacuoles were also recognized (arrowhead). **C** and **F**, EMPA + S/V group showed a lower number of granules. However, there was a general view of healthy cell structure. **D** and **G**, S/V group had also a lower number of granules. Although some cells were seen with a large number of vacuoles (**D**), ultrastructural observations showed that the organelles were not damaged. EMPA: Empagliflozin; S/V: Sacubitril/valsartan. Nc: Nucleus.

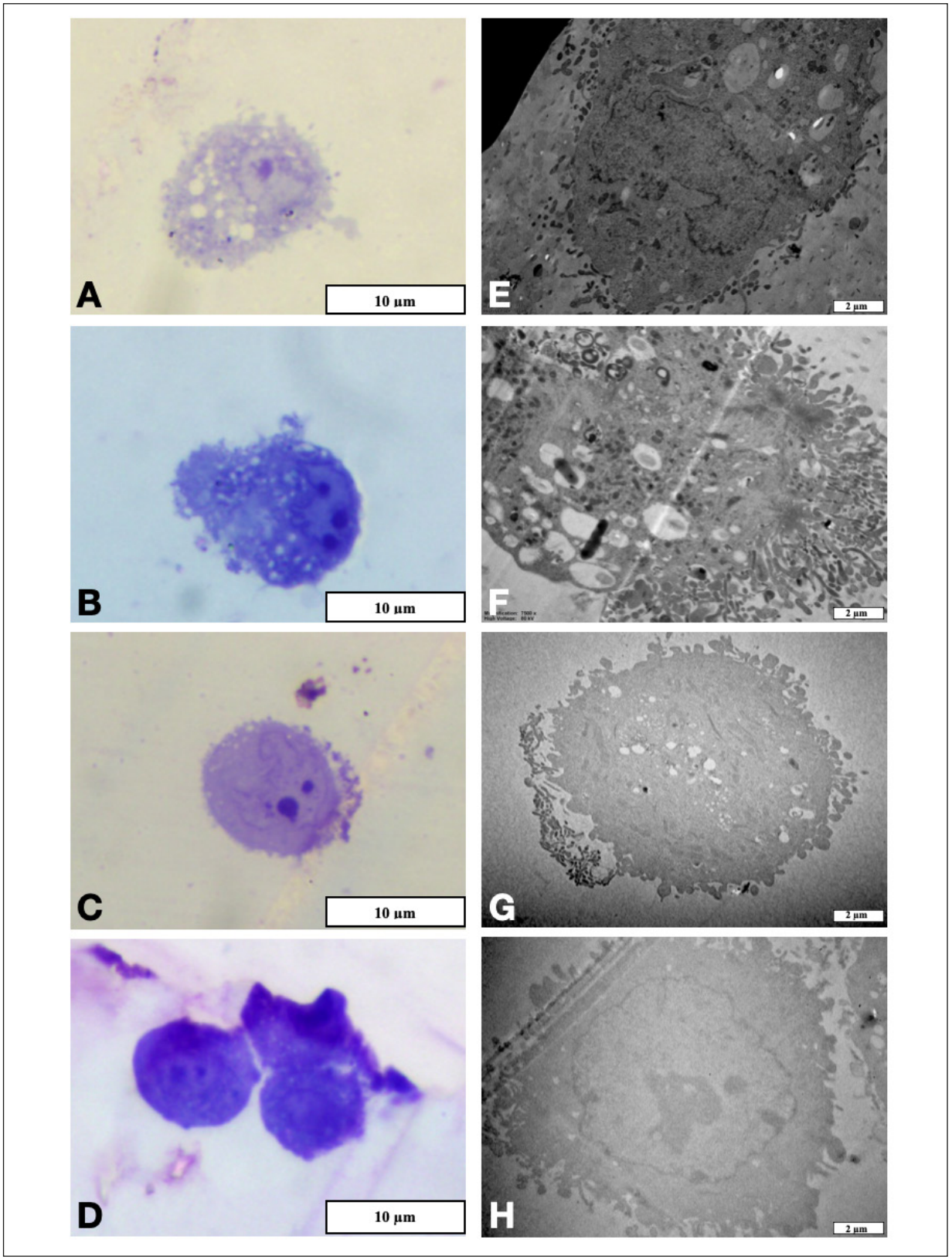

Figure 6. Representative micrographs from semi-thin (**A-D**) and thin (**E-H**) sections of the H9C2 (2-1) cardiomyocyte cell line. **A** and **E**, MTX group. **B** and **F**, MTX + EMPA group. **C-G**, MTX + S/V group. **D-H**, MTX + EMPA + S/V group. MTX: Methotrexate; EMPA: Empagliflozin; S/V: Sacubitril/valsartan.

life. Previous studies[35,36] have shown that HIF-1α-/- mouse embryos stop developing in the middle of gestation and die as a result of cardiovascular defects and decreased erythropoiesis. These findings prove that the development of all three components of the circulatory system is dependent on the HIF-1α molecule[37]. In the current study, S/V and EMPA treatment attenuated MTX-induced hypoxia by reducing HIF-1α levels. This effect may be further enhanced with S/V therapy rather than combined therapy. A negative correlation was found between HIF-1α and TAC in cells receiving S/V treatment. The primary underlying protective mechanism of S/V was mediated by the inhibition of the oxidative stress/HIF-1α signaling pathway. EMPA treatment at high concentrations of glucose may also play an important role in protecting against proximal renal tubular cell damage and the induction of HIF-lα expression by EMPA, in the protection of high glucose-induced proximal renal tubular epithelial cell damage[38]. Suematsu et al[39] investigated the effects and mechanisms of angiotensin receptor-neprilysin inhibitors (ARNis) in HF with decreased ejection fraction in diabetic mice. S/V is also an angiotensin receptor/neprilysin inhibitor that has significantly reduced the rates of cardiovascular death or hospitalization for HF and improved functional status in patients with chronic heart failure, reduced LV ejection fraction, compared to other drugs[40-42]. It is seen that *in vivo* studies will shed further light on clinical applications by providing a more detailed understanding of the subject.

Cardiovascular diseases (CVD) are playing an increasing role as a major cause of mortality and morbidity worldwide. Atherosclerosis alone accounts for more than half of all deaths in the western world. Various hypotheses[43] have been proposed regarding the pathogenesis of atherosclerosis. The most valid pertains to the oxidative stress. According to this hypothesis, macrophage polarization, caused by the imbalance between oxidant/antioxidant factors, leads to the formation of atherogenic plaques[43]. Oxidative stress has been identified[44] as an important pathophysiological pathway in the development and progression of HF. In the current study, MDA, LOOH, AOPP, and XO activity were increased while T-SH, CAT and TAC levels were decreased in MTX-induced H9c2 cardiomyocyte cells. Today, it is often difficult to predict which patients will benefit most from different treatments. Perhaps when we pay attention to the aberrations in redox biomarkers, this may help us to qualify patients for the use of S/V and EMPA. Although there is evidence from clinical and animal studies[11-18] that S/V and EMPA have many positive effects on CVD. These studies cannot show whether these therapies have a direct protective effect on cardiomyocytes. While S/V and EMPA inhibited the production of oxidant (MDA, LOOH, AOPP, XO) molecules, they increased the activity of antioxidant (T-SH, CAT, TAC) molecules. Especially the combined use of S/V and EMPA was more effective on these molecules. Our study suggests that chronic oxidative stress contributes to smooth muscle cells (SMC) proliferation and migration, and that S/V and EMPA attenuate these effects. In MI-induced rats, resveratrol, S/V, and valsartan prevented cardiac remodeling and dysfunction by reducing oxidative stress, inflammation and fibrosis[45]. S/V significantly prevented the degradation of antioxidant enzymes (SOD, CAT, GR, GPx, GST, and GSH) and increased MDA levels in Wistar rats induced by isoproterenol (ISO) poisoning. Inhibition of enzyme neprilysin alleviated the ISO-induced myocardial damage mediated by its strong antioxidant potential[16]. Our study joins previous studies[16,45-49] in demonstrating that treatment with S/V involves an improvement in antioxidant status and reduces the oxidative stress, inflammation and apoptotic pathway to improve the cardiac function. EMPA has been shown to reduce cardiac fibrosis and oxidative stress in a diabetic mouse model[13]. Barış et al[50] suggest that lower antioxidant levels, which is an indicator of the damage caused by reactive oxygen metabolites, and the lack of improvement in these parameters in the EMPA group reveal that this effect of the healing occurs independently of antioxidant pathways. EMPA exerted beneficial antioxidant, anti-inflammatory, anti-mitogenic and anti-migratory effects under normal glucose conditions and without inducing cell death. These results highlight the therapeutic potential of EMPA in vascular proliferative diseases. EMPA significantly prevents acute cardiotoxicity induced by multiple pathways, both antioxidant and non-antioxidant, as in our study[47-53].

Limitations of the Study

Although our study has strengths, it has some limitations. The results of our study should have been supported by *in vivo* animal and human studies. Other markers to support ischemia could be studied.

Conclusions

The results of this study performed with S/V and EMPA under *in vitro* conditions indicate that these molecules may boast protective effects on the mechanical activity of the heart by affecting more than one intracellular pathway (oxidative stress and HIF-1a) in cardiac dysfunction. The data obtained from the study show that besides the protective effect of S/V and EMPA, hypoxia and antioxidant effects, especially the increase in S/V cytoplasmic vacuoles and peripherally elongated located mitochondrial biogenesis prevents degeneration in cardiomyocytes. Our findings suggest that S/V and EMPA are beneficial and may be further explored for their clinical efficacy in the setting of CVD in future clinical trials.

Availability of Data and Materials

The data underlying this article are available in the article. If needed, please contact the corresponding author. The email address is drzeki@yahoo.com

Ethics Approval

Ethics Committee approval is not required for cell culture studies.

Informed Consent

Informed consent is not required for cell culture studies.

Funding

None.

Conflict of Interest

The authors declare that they have no conflict of interest.

Authors' Contributions

ZD, AS and HU participated in the design of the study. DDE studied cell culture. HS and GES studied the cells under the electron microscope. SD, RG and HU carried out the ELISA and spectrofotometric test. SD performed the statistical analysis. ZD, AS and HU wrote the paper. All of authors made the revisions and performed final proofreading.

ORCID ID

Zeki Doğan: 0000-0002-5620-7268

References

1) Rocca A, Heeswijk RBV, Richiardi J, Meyer P, Hullin R. The Cardiomyocyte in Heart Failure with Preserved Ejection Fraction-Victim of Its Environment? Cells 2022; 11: 867.
2) Docherty KF, Vaduganathan M, Solomon SD, McMurray JJV. Sacubitril/Valsartan: Neprilysin Inhibition 5 Years After PARADIGM-HF [published correction appears in JACC Heart Fail 2020; 8: 1057]. JACC Heart Fail 2020; 8: 800-810.
3) Isaji M. Sodium-glucose cotransporter inhibitors for diabetes. Curr Opin Investig Drugs 2007; 8: 285-292.
4) Cosentino F, Grant PJ, Aboyans V, Bailey CJ, Ceriello A, Delgado V, Federici M, Filippatos G, Grobbee DE, Hansen TB, Huikuri HV, Johansson I, Jüni P, Lettino M, Marx N, Mellbin LG, Östgren CJ, Rocca B, Roffi M, Sattar N, Seferović PM, Sousa-Uva M, Valensi P, Wheeler DC; ESC Scientific Document Group. 2019 ESC Guidelines on diabetes, pre-diabetes, and cardiovascular diseases developed in collaboration with the EASD. Eur Heart J 2020; 41: 255-323.
5) Weidemann A, Johnson RS. Biology of HIF-1α. Cell Death Differ 2008; 15: 621-627.
6) Semenza GL. Oxygen sensing, homeostasis, and disease. New Engl J Med 2011; 365: 537-547.
7) Senoner T, Dichtl W. Oxidative Stress in Cardiovascular Diseases: Still a Therapeutic Target? Nutrients 2019; 11: 2090.
8) Romão PVM, Palozi RAC, Guarnier LP, Silva AO, Lorençone BR, Nocchi SR, Moura CCFS, Lourenço ELB, Silva DB, Gasparotto Junior A. Cardioprotective effects of Plinia cauliflora (Mart.) Kausel in a rabbit model of doxorubicin-induced heart failure. J Ethnopharmacol 2019; 242: 112042.
9) Trivedi RK, Polhemus DJ, Li Z, Yoo D, Koiwaya H, Scarborough A, Goodchild TT, Lefer DJ. Combined Angiotensin Receptor-Neprilysin Inhibitors Improve Cardiac and Vascular Function Via Increased NO Bioavailability in Heart Failure. J Am Heart Assoc 2018; 7: e008268.
10) Szczurek W, Szyguła-Jurkiewicz B. Oxidative stress and inflammatory markers - the future of heart failure diagnostics? Kardiochir Torakochirurgia Pol 2015; 12: 145-149.
11) Yu C, Li D, Li Z, Yu D, Zhai G. Effect of sacubitril/valsartan on inflammation and oxidative stress in doxorubicin-induced heart failure model in rabbits. Acta Pharm 2020; 71: 473-484.
12) Kolijn D, Pabel S, Tian Y, Lódi M, Herwig M, Carrizzo A, Zhazykbayeva S, Kovács Á, Fülöp GÁ, Falcão-Pires I, Reusch PH, Linthout SV, Papp Z, van Heerebeek L, Vecchione C, Maier LS, Ciccarelli M, Tschöpe C, Mügge A, Bagi Z, Sossalla S, Hamdani N. Empagliflozin improves endothelial and cardiomyocyte function in human heart failure with preserved ejection fraction via reduced pro-inflammatory-oxidative pathways and protein kinase Gα oxidation. Cardiovasc Res 2021; 117: 495-507.

13) Li C, Zhang J, Xue M, Li X, Han F, Liu X, Xu L, Lu Y, Cheng Y, Li T, Yu X, Sun B, Chen L. SGLT2 inhibition with empagliflozin attenuates myocardial oxidative stress and fibrosis in diabetic mice heart. Cardiovasc Diabetol 2019; 18: 15.

14) Butler J, Filippatos G, Siddiqi TJ, Ferreira JP, Brueckmann M, Bocchi E, Böhm M, Chopra VK, Giannetti N, Iwata T, Januzzi JL, Kaul S, Piña IL, Ponikowski P, Rauch-Kröhnert U, Shah SJ, Senni M, Sumin M, Verma S, Zhang J, Pocock SJ, Zannad F, Packer M, Anker SD. Effects of Empagliflozin in Women and Men with Heart Failure and Preserved Ejection Fraction. Circulation 2022; 146: 1046-1055.

15) Zou R, Shi W, Qiu J, Zhou N, Du N, Zhou H, Chen X, Ma L. Empagliflozin attenuates cardiac microvascular ischemia/reperfusion injury through improving mitochondrial homeostasis. Cardiovasc Diabetol 2022; 21: 106.

16) Imran M, Hassan MQ, Akhtar MS, Rahman O, Akhtar M, Najmi AK. Sacubitril and valsartan protect from experimental myocardial infarction by ameliorating oxidative damage in Wistar rats. Clin Exp Hypertens 2019; 41: 62-69.

17) Jing W, Vaziri ND, Nunes A, Suematsu Y, Farzaneh T, Khazaeli M, Moradi H. LCZ696 (Sacubitril/valsartan) ameliorates oxidative stress, inflammation, fibrosis and improves renal function beyond angiotensin receptor blockade in CKD. Am J Transl Res 2017; 9: 5473-5484.

18) Uthman L, Li X, Baartscheer A, Schumacher CA, Baumgart P, Hermanides J, Preckel B, Hollmann MW, Coronel R, Zuurbier CJ, Weber NC. Empagliflozin reduces oxidative stress through inhibition of the novel inflammation/NHE/[Na+]c/ROS-pathway in human endothelial cells. Biomed Pharmacother 2022; 146: 112515.

19) Slater TF, Sawyer B, Straeulı U. Studıes on succınate-tetrazolıum reductase systems. III. poınts of couplıng of four dıfferent tetrazolıum salts. Biochim Biophys Acta 1963; 77: 383-393.

20) Berridge MV, Tan AS. Characterization of the cellular reduction of 3-(4,5-dimethylthiazol-2-yl)-2,5-diphenyltetrazolium bromide (MTT): subcellular localization, substrate dependence, and involvement of mitochondrial electron transport in MTT reduction. Arch Biochem Biophys 1993; 303: 474-482.

21) Buege JA, Aust SD. Microsomal lipid peroxidation. Meth Enzymol 1978; 52: 302-310.

22) Jiang ZY, Hunt JV, Wolff SP. Ferrous ion oxidation in the presence of xylenol orange for detection of lipid hydroperoxide in low density lipoprotein. Anal Biochem 1992; 202: 384-389.

23) Gelisgen R, Genc H, Kayali R, Oncul M, Benian A, Guralp O, Uludag S, Cakatay U, Albayrak M, Uzun H. Protein oxidation markers in women with and without gestational diabetes mellitus: a possible relation with paraoxonase activity. Diabetes Res Clin Pract 2011; 94: 404-409.

24) Prajda N, Weber G. Malignant transformation-linked imbalance: decreased xanthine oxidase activity in hepatomas. FEBS letters 1975; 59: 245-249.

25) Hu ML. Measurement of protein thiol groups and glutathione in plasma. Methods Enzymol 1994; 233: 380-385.

26) Yasmineh WG, Kaur TP, Blazar BR, Theologides A. Serum catalase as marker of graft-vs-host disease in allogeneic bone marrow transplant recipients: pilot study. Clin Chem 1995; 41: 1574-1580.

27) Benzie IF, Strain JJ. The ferric reducing ability of plasma (FRAP) as a measure of ""antioxidant power": the FRAP assay". Anal Biochem 1996; 239: 70-76.

28) McMurray JJ, Packer M, Desai AS, Gong J, Lefkowitz MP, Rizkala AR, Rouleau JL, Shi VC, Solomon SD, Swedberg K, Zile MR; PARADIGM-HF Investigators and Committees. Angiotensin-neprilysin inhibition versus enalapril in heart failure. N Engl J Med 2014; 371: 993-1004.

29) Riggs K, Ali H, Taegtmeyer H, Gutierrez AD. The Use of SGLT-2 Inhibitors in Type 2 Diabetes and Heart Failure. Metab Syndr Relat Disord 2015; 13: 292-297.

30) Andreadou I, Efentakis P, Balafas E, Togliatto G, Davos CH, Varela A, Dimitriou CA, Nikolaou PE, Maratou E, Lambadiari V, Ikonomidis I, Kostomitsopoulos N, Brizzi MF, Dimitriadis G, Iliodromitis EK. Empagliflozin Limits Myocardial Infarction in Vivo and Cell Death in Vitro: Role of STAT3, Mitochondria, and Redox Aspects. Front Physiol 2017; 8: 1077.

31) Liu X, Li D, Pi W, Wang B, Xu S, Yu L, Yao L, Sun Z, Jiang J, Mi Y. LCZ696 protects against doxorubicin-induced cardiotoxicity by inhibiting ferroptosis via AKT/SIRT3/SOD2 signaling pathway activation. Int Immunopharmacol 2022; 113: 109379.

32) Jiang BH, Semenza GL, Bauer C, Marti HH. Hypoxia-inducible factor 1 levels vary exponentially over a physiologically relevant range of O2 tension. Am J Physiol 1996; 271: C1172-C1180.

33) Jewell UR, Kvietikova I, Scheid A, Bauer C, Wenger RH, Gassmann M. Induction of HIF-1alpha in response to hypoxia is instantaneous. FASEB J 2001; 15: 1312-1314.

34) Yu AY, Frid MG, Shimoda LA, Wiener CM, Stenmark K, Semenza GL. Temporal, spatial, and oxygen-regulated expression of hypoxia-inducible factor-1 in the lung. Am J Physiol 1998; 275: L818-L826.

35) Compernolle V, Brusselmans K, Franco D, Moorman A, Dewerchin M, Collen D, Carmeliet P. Cardia bifida, defective heart development and abnormal neural crest migration in embryos lacking hypoxia-inducible factor-1alpha. Cardiovasc Res 2003; 60: 569-579.

36) Yoon D, Pastore YD, Divoky V, Liu E, Mlodnicka AE, Rainey K, Ponka P, Semenza GL, Schumacher A, Prchal JT. Hypoxia-inducible factor-1 deficiency results in dysregulated erythropoiesis signaling and iron homeostasis in mouse development. J Biol Chem 2006; 281: 25703-25711.

37) Semenza GL. Oxygen sensing, homeostasis, and disease. New Engl J Med 2011; 365: 537-547.

38) Ndibalema AR, Kabuye D, Wen S, Li L, Li X, Fan Q. Empagliflozin Protects Against Proximal Renal Tubular Cell Injury Induced by High Glucose via Regulation of Hypoxia-Inducible Factor 1-Alpha. Diabetes Metab Syndr Obes 2020; 13: 1953-1967.

39) Suematsu Y, Miura S, Goto M, Matsuo Y, Arimura T, Kuwano T, Imaizumi S, Iwata A, Yahiro E, Saku K. LCZ696, an angiotensin receptor-neprilysin inhibitor, improves cardiac function with the attenuation of fibrosis in heart failure with reduced ejection fraction in streptozotocin-induced diabetic mice. Eur J Heart Fail 2016; 18: 386-393.

40) Lamendola P, Lanza GA, Melita V, Villano A, Palermo C, Leone D, Lombardo A, Pennestrì F, Crea F, Mercuri EM, Pane M. Duchenne muscular dystrophy: preliminary experience with sacubitril-valsartan in patients with asymptomatic left ventricular dysfunction. Eur Rev Med Pharmacol Sci 2020; 24: 9112-9115.

41) Monzo L, Gaudio C, Cicogna F, Tota C, Petronilli V, Mennuni S, De Ruvo E, Calò L. Impact of sacubitril/valsartan on implantable defibrillator eligibility in heart failure: a real-world experience. Eur Rev Med Pharmacol Sci 2021; 25: 5690-5700.

42) Monzo L, Gaudio C, Cicogna F, Tota C, Petronilli V, Mennuni S, De Ruvo E, Calò L. Author Correction: Impact of sacubitril/valsartan on implantable defibrillator eligibility in heart failure: a real-world experience. Eur Rev Med Pharmacol Sci 2022; 26: 2216.

43) Khosravi M, Poursaleh A, Ghasempour G, Farhad S, Najafi M. The effects of oxidative stress on the development of atherosclerosis. Biol Chem 2019; 400: 711-732.

44) van der Pol A, van Gilst WH, Voors AA, van der Meer P. Treating oxidative stress in heart failure: past, present and future. Eur J Heart Fail 2019; 21: 425-435.

45) Raj P, Sayfee K, Parikh M, Yu L, Wigle J, Netticadan T, Zieroth S. Comparative and Combinatorial Effects of Resveratrol and Sacubitril/Valsartan alongside Valsartan on Cardiac Remodeling and Dysfunction in MI-Induced Rats. Molecules 2021; 26: 5006.

46) Yu C, Li D, Li Z, Yu D, Zhai G. Effect of sacubitril/valsartan on inflammation and oxidative stress in doxorubicin-induced heart failure model in rabbits. Acta Pharm 2020; 71: 473-484.

47) Dindaş F, Güngör H, Ekici M, Akokay P, Erhan F, Doğduş M, Yılmaz MB. Angiotensin receptor-neprilysin inhibition by sacubitril/valsartan attenuates doxorubicin-induced cardiotoxicity in a pretreatment mice model by interfering with oxidative stress, inflammation, and Caspase 3 apoptotic pathway. Anatol J Cardiol 2021; 25: 821-828.

48) Hou M, Lu L, Wu X, Liu H. LCZ696 Ameliorates Isoproterenol-Induced Acute Heart Failure in Rats by Activating the Nrf2 Signaling Pathway. Appl Bionics Biomech 2022; 2022: 6077429.

49) Peng S, Lu XF, Qi YD, Li J, Xu J, Yuan TY, Wu XY, Ding Y, Li WH, Zhou GQ, Wei Y, Li J, Chen SW, Liu SW. LCZ696 Ameliorates Oxidative Stress and Pressure Overload-Induced Pathological Cardiac Remodeling by Regulating the Sirt3/MnSOD Pathway. Oxid Med Cell Longev 2020; 2020: 9815039.

50) Barış VÖ, Dinçsoy AB, Gedikli E, Zırh S, Müftüoğlu S, Erdem A. Empagliflozin Significantly Prevents the Doxorubicin-induced Acute Cardiotoxicity via Non-antioxidant Pathways. Cardiovasc Toxicol 2021; 21: 747-758.

51) Sukhanov S, Higashi Y, Yoshida T, Mummidi S, Aroor AR, Jeffrey Russell J, Bender SB, DeMarco VG, Chandrasekar B. The SGLT2 inhibitor Empagliflozin attenuates interleukin-17A-induced human aortic smooth muscle cell proliferation and migration by targeting TRAF3IP2/ROS/NLRP3/Caspase-1-dependent IL-1β and IL-18 secretion. Cell Signal 2021; 77: 109825.

52) Li N, Zhou H. SGLT2 Inhibitors: A Novel Player in the Treatment and Prevention of Diabetic Cardiomyopathy. Drug Des Devel Ther 2020; 14: 4775-4788.

53) Gohari S, Reshadmanesh T, Khodabandehloo H, Karbalaee-Hasani A, Ahangar H, Arsang-Jang S, Ismail-Beigi F, Dadashi M, Ghanbari S, Taheri H, Fathi M, Muhammadi MJ, Mahmoodian R, Asgari A, Tayaranian M, Moharrami M, Mahjani M, Ghobadian B, Chiti H, Gohari S. The effect of EMPAgliflozin on markers of inflammation in patients with concomitant type 2 diabetes mellitus and coronary artery disease: the EMPA-CARD randomized controlled trial. Diabetol Metab Syndr 2022; 14: 170.